MSc Dissertation
Final Report
MSc in Integrated Machine Learning Systems

Student: Sebastian Barrera Parissaki

Student number: 19162034

Project Title:

Motion sensing for medical applications with FMCW radar

Supervisor: Dr. Matthew Ritchie

University College London

Dept. of Electronic and Electrical Engineering

2020-21

Abstract

This project focuses on taking radar data and analysing it in order to classify the movement happening as one of a set of classes. The pre-processing step includes using an MTI filter to remove static objects in the background and compiling a spectrogram of the target movement as Doppler vs time. This final spectrogram is used to extract features and classify it. A feedback loop is included to try and improve the accuracy, where the parameters of the filter and spectrogram are changed, as well as the feature extraction, based on the increase or decrease of accuracy when measuring against a baseline model. The final model achieves a 92.3% accuracy, slightly higher than using deep learning, which provides 91%.

The conclusions of this task are used to propose a system to track and evaluate the movement of patients. A baseline movement is created for every person based on how the move normally, which is then used to compare against every instance of a new movement. Features are extracted from the way the person moves and feedback is given as to how different a new instance might be from the baseline. A custom dataset is created with 8 people doing three activities (walking, sitting down and standing up) and variations of these in order to compare them with the baseline movement. If the patient is walking and an irregularity in the movement is detected, a model classifies the movement as one of 6 walks that are associated with gait diseases, being able to detect if the patient could be suffering from one of them, with an accuracy of 99%.

Contents

1. Introduction

Radars are becoming more and more popular in applications where the purpose is to monitor vital signs or detect if a fall has occurred. Clearly, both these cases have extensive medical applications, from unobtrusive sensing [1] to detecting if patients at a care home have fallen over in their room [2]. Most studies focus on classifiers that estimate if there was a fall or not, or in other cases, they classify the movement as one of n labels. However, there is a largely unexplored area that involves the monitoring of the movement of patients with a radar. The difference here is that monitoring implies a continued observation to analyse the evolution of a patient. With this being the ultimate aim of the project, it will be divided into two parts:

A) Classify a movement

This project will explore signals obtained from radar signatures of moving objects. In this case, the objects are people who are performing a set of movements, namely six: walking, sitting down, standing up, bending down, drinking water and falling.

The university of Glasgow has made available a dataset [3] with these six movements recorded on multiple patients with a few repetitions of each. The first objective of the project will be to classify these movements correctly. For this purpose, features should be extracted from the spectrogram or the range-time plot. For this to be possible, an MTI filter will be applied to the input signals, later creating the spectrogram. Figure 1 shows example spectrograms for all six possible movements.

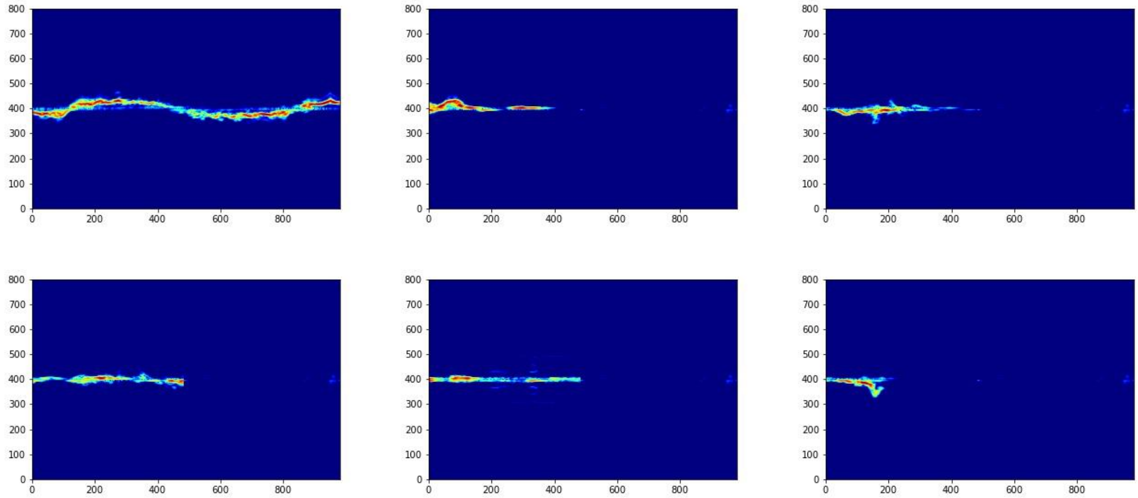

Figure 1: Movements in order from top left to bottom right: Walking, Sitting, Standing up, Bending down, Drinking water, Falling

The purpose of this first part of the project is to extract information to later be used on a dataset created by the student, which will focus on the second part of the project. The main questions this part aims to answer are things like what features work best on the spectrogram, what are the parameters that provide the best accuracy, what is the purpose of the MTI filter… With these questions answered, the second part of the project will be much more streamlined and can focus on other aspects.

B) Evaluate a movement

The novel aspect that this project aims to introduce is to have a personalized system that can recognise the movement a person is making and evaluate it against a baseline. Since there is no dataset large enough to carry this out, one is created by capturing data with an Ancortek radar. This dataset contains three movements (walking, sitting down and standing up) of eight people, and variations of these movements. These variations will be compared to the baseline and assessed to try and identify what the problem might be. Every person will have their own baseline movement to be compared against, offering feedback of how every instance of movement differs from their “normal” movement.

The applications that this could have are:

- At home monitoring: people in care homes to monitor their state.
- Athletes: A slight change in movement could indicate an overcharged joint or the possibility of a future injury. This system could also be used to track the progress of an athlete doing an activity (a footballer could asses if he is improving at shooting).
- Physiotherapy: Patients won’t have to visit the doctor to assess their progress, but could do it at home with a radar that tells them how “normal” their movement is.
- Diseases: The most common gait diseases could be identified in radar signals and they could be used to diagnose patients.

2. Background Theory and literature review

Radar is a detection system based on propagating waves through the air and then receiving the returning signals (returning as the bounce off objects) and with this information compute the objects' location and speed. The foundation of pulse radar was during WWII, using waves with a narrow band and high energy. It wasn't until the 1970s that it was considered using radars for medical sensing. What made radar lend itself for medical sensing is that it has the ability to extract information from a complex structure such as the human body. CW radars were used to detect heart rate and breathing rate in the 80s, but it was in the 90 that Thomas E. McEwan registered a patent for the Microwave Impulse Radar (MIR) [4], which employs very short pulses of 200ps, and therefore a large bandwidth. With this, sensing the range of objects became possible with radars, as CW radars were only able to detect velocity [5].

2.1. Background theory

The applications of radar throughout history and nowadays are unlimited. The main focus of the project is the application of these techniques for medical sensing, so only findings in this area will be reviewed. Figure 2 shows a simplified diagram for how a radar works.

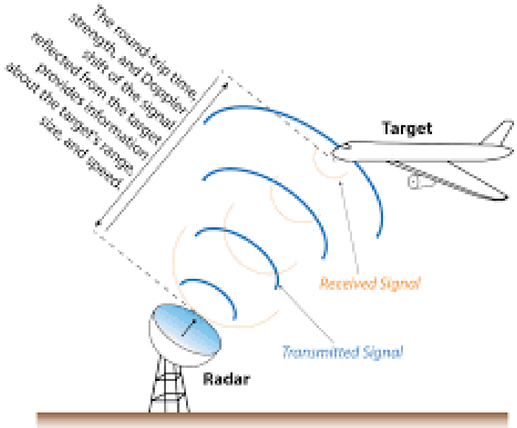

Figure 2: Functioning of radar

Radars for monitoring physiologic functions started in the 1970s, but it was too expensive and cumbersome. Nowadays, three of them are the most used: CW, UWB (ultrawideband) and FMCW [6].

2.1.1. UWB

UWB generates a square wave with a repetition rate in 0.05-30MHz range. The signal is radiated and then captured by the receiving antenna. A delayed copy of the radiated signal is used to drive a strobe pulse generator which serves as a sampling signal for the receiver. If this is delayed by the same amount of time that it takes for the signal to be captured by the receiving antenna, the signal is sampled at its maximum amplitude and integrated over successive pulses. They can be used for medical imaging and for heart rate and pulmonary motion monitoring. These radars have the following advantages: enhanced capability to penetrate through obstacles, high precision ranging, low electromagnetic radiation and small size and power.

2.1.2. CW

CW transmits a continuous wave with a stable frequency [7]. They are simpler to fabricate than the UWB radars and have no minimum and maximum range, although there is a practical range imposed by the broadcast power level. The downside is that they are not able to detect range of objects, only speed. Speed can be detected by a direct measurement of the Doppler Shift of the return signal. The

Doppler shift works as a change in frequency of the wave caused by a motion relative to the transmitter, which means it can either be the transmitter moving or it can be the target. If the relative movement is the receiver moving opposite to the direction of propagation, the wavelength would be reduced, which causes an increase in frequency. If the receiver is moving in the direction of propagation, the frequency will decrease. Figure 3 shows this principle.

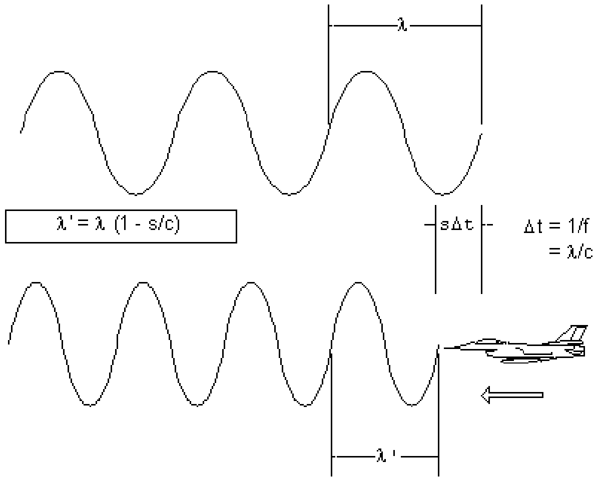

Figure 3: Doppler shift

2.1.3. FMCW

FMCW works a similar way as CW, but the frequency can be modulated, allowing for range to be detected [8]. The emitted signal is a constant amplitude sinewave whose frequency is modulated as a sawtooth signal. The frequency of the received signal when comparing to the emitted one offers information on the position and velocity of the objects. Figure 4 shows a simplified graph.

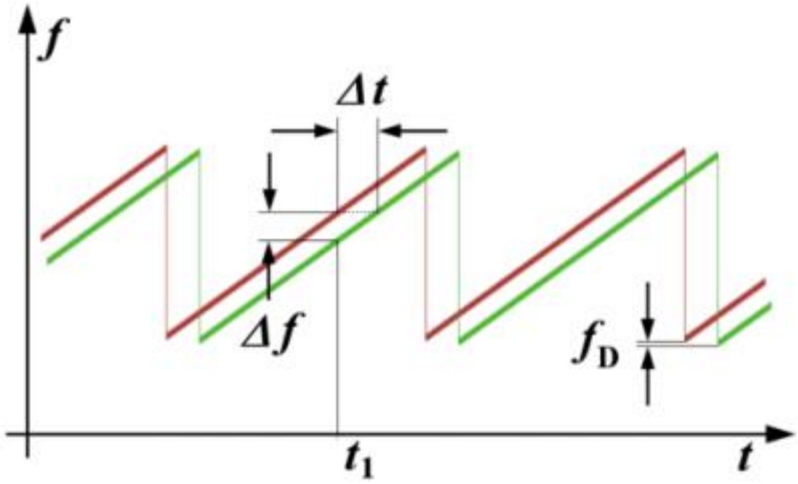

Figure 4: FMCW signal

Red is the emitted signal and green is the received. Δt is a measure of the distance between emitter and obstacle, while f_D measures the velocity at which the obstacle is moving away. However, this figure is a simplification, and in practice the received signal is very complex, as there are many sources of reflections.

2.2. Literature review

2.2.1. UWB

The applications of UWB radars are [9] [10]:

1. Medical monitoring: detecting movement of a person in a room, and after processing the signal to analyse the situation of people in the room. In a larger scale, more UWB radars should be used, since their range is only 10 meters, but since the precision is very high, it could even be used to monitor the breathing of patients.
2. Medical imaging: Since the electromagnetic pulses are able to penetrate the body, the radar can non-invasively detect movements of organs. Figure 5 (taken from [9]), shows the attenuation of the signal depending on the depth. The UWB radar could be used to detect cardiac contractions, arterial wall motion and respiratory movements.

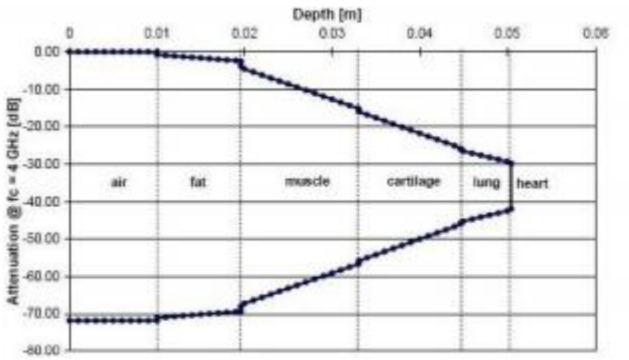

Figure 5: Attenuation of UWB signal

Another application in the medical imaging domain is to monitor the last period of pregnancy.

2.2.2. CW

An application is for pregnancy monitoring, being one of the most used technologies in clinical practices [11]. However, they are not used as commonly as the other two types in the medical domain, since they can be used for unobtrusive vitals monitoring, but the signal detects many movements: respiration, blood circulation and even regular movement. To distinguish these, range information is needed, which is why the FMCW radar is much more common. [12] explores how this type of radar can be used to recognize humans by estimating their gait.

2.2.3. FMCW

An application of the FMCW radar is sensing with microwave doppler radar for unobtrusive sensing. For this type of sensing, since the skin reflects 99% of the ultrasound wave, there must be contact between the transmitter and receiver with the skin, and also no air bubbles in between them. If these conditions are met, and a wave-conducting gel is applied to the area of the body, the radar can detect the position and movement of organs inside the body.

The project in hand will focus on motion sensing with the FMCW radar. Previous work in motion sensing with FMCW radar is:

- A paper from 2018 [13] focuses on hand gesture recognition at a medium range, pre-processing the signal and using CNNs to predict the hand movement.
- A paper from 2017 [14] focuses on hand gesture recognition again, but this time in the presence of multiple targets. Its findings show that the radar can be used for gesture recognition even in the presence of other moving people.
- An older paper from 2010 [15] uses FMCW radars for pervasive health care monitoring, using radars around the house to sense the heart rate and breath rate.

2.2.4. Applications

After explaining the focus of every type of radar, it is important to evaluate what products or studies have been made in the application domain that the project will focus on.

2.2.4.1. At-home monitoring

1. Wearables:

Some examples of proposed wearables are:

i. A paper from 2015 [16], which proposes an affordable wristband to monitor scenarios for conditions that elderly people can suffer from that might impair their independence. It can detect Parkinson's, dementia…
ii. A paper from 2019 [17] uses a wristband to detect arthritis in patients, but also implements an IoT solution for obtaining and storing the data.
iii. Many products are available in the market, such as the MobileHelp Smart, which monitors the health of the patients and can create alerts if it detects a problem. Another product is something as popular as the Apple Watch, which can keep track of the vitals, but is not specifically designed for monitoring the elderly.

All these devices and products are very different from the proposed system, since it will be based on radar. In any case, it is valuable in order to guide the project in a specific direction. The main takeaway is that much research has been done in vitals detection, and using a radar for this might be unwise, since other solutions already exist in the wearables domain.

2. Ambient solutions: many products are available; two examples are detailed below:

i. Alarm Wellness: product to completely monitor people at home. It includes door sensors, motion sensors, wearables, cameras…etc. Apart from the fact that the cameras pose privacy concerns, and the fact that wearables might be uncomfortable, the solution proposed is much simpler and cheaper.
ii. Rest Assured: sensors and cameras, suffers from the same problems as the previous solution. However, privacy concerns are addressed by offering a dedicated safe portal to monitor the patients.

These are complete systems that require a lot of setting up and create massive amount of data. The proposed system is focused on using a single radar to be able to detect the movement of the people and learn it. For the purpose of the project, these systems are overly complicated and offer too much information.

3. Radar-based: A great amount of effort has been focused on hand gestures and vital monitoring, but not as much on whole body movement or disease detection.

i. A paper from 2017 [18] shows a very complete study, where the movement is detected as well as the vital signals. However, the detection of movement is focused on fall detection, and not in general classification of movements. Apart from this, a UWB radar is used, which has less range and accuracy than the FMCW [19].
ii. A paper from 2012 [20] detects if the patients inside a care home are walking, but it does not do anything with that information. No disease detection, no difference in walks… Another paper from 2018 [21] measures the gait speed, and mentions that a decrease can cause falls, but does not implement an algorithm to take this into account.
iii. Many more papers focused on fall detection [22] [23] [24], and therefore this a domain that will not be studied, since many studies have already been done on the subject.

Overall, it is clear that many solutions have been offered in this domain, mainly wearables. Ambient solutions are not comparable to the work proposed for this project, as they use many more sensors and are complex systems. For the comparable work that has already been done, the main takeaway is that fall detection has been greatly studied, and therefore will not be explored.

2.2.4.2. Athletes

A paper from 2021 [25] shows that a micro doppler radar can detect slight changes in movement that would not be measured by image processing techniques. This is tested by sensing athletes jumping barefoot, with shoes and with a heel lift, and the algorithm being able to correctly classify them. One of the future work proposals is to study if the signals can be used to identify pathologic movement patterns or risk of injury.

As said before, very little work has been done with radars in detecting athlete injuries. However, many wearable technologies are available to monitor their health.

- A paper from 2003 [26] proposes a platform with three subparts: athlete, rehabilitation and portal. Athlete records all the sensor readings and offer information to the athletes about their performance and habits. Rehabilitation provides alerts and decision support mechanisms to predict and prevent injuries. The portal is a historical database with data.
- A paper from 2019 [27] proposes a wearable sensor that can also monitor saliva excretion or sweat to offer more features for the algorithm to offer feedback to the athletes.
- A paper from 2017 [28] explains the limitations of these wearable devices, like the inability to track position, movement, velocity… etc; and provides ideas for dealing with these limitations.

This last paper sums up many of the reasons why radar can provide better results than wearable technologies. Although monitoring the vitals of athletes is very valuable, the information taken from the radar could provide a much clearer view of their movement patterns. When these patterns change, that indicates risk and a possible injury. What makes radar better in this case than going to the doctor is that the doctor will have to perhaps run many tests to assess if there is any problem (x-ray, MRI…), while the radar has proved that it can detect very slight changes in movement, and therefore it could "see" things invisible to the naked eye, even to a trained professional.

2.2.4.3. Physiotherapy

A paper from 2017 [29] Provides a detailed study into how a radar system can help with upper or lower limbs physiotherapy recovery. It also gives an overview of other unobtrusive and remote systems that can offer input, such as thermography or cameras. A paper from 2013 [30] uses image processing techniques to assess the state of recovery. A paper from 2020 [31] shows a wearable technology to track physiotherapy recovery in rotator cuff pathology.

Overall, this is a fairly unexplored area, and while some advances have been made with image processing and wearables, it is considered that a radar system lends itself very well to tracking the recovery of patients. The price and usability of the technology works in its favor to deliver satisfactory results, along with the fact that it can detect slight changes in movement patterns, which could indicate an improvement in the recovery.

2.2.4.4. Diseases

Gait has been estimated in many papers to try and classify instances with different labels. A paper from 2017 [32] features a detailed study of gait classification for three groups: young, elderly and elderly with a history of falling. The study was successful in recognizing a certain person by their gait pattern. However, this study did not check for gait abnormalities and diseases that they could indicate. Another paper from 2016 [33] also classifies different gaits: walking without a bag, with bag on one hand or bag in two hands.

As for using it for detecting diseases, not much work has been done. A paper from 2019 [34] uses not only gait velocity, but also leg and foot movement to try and detect diseases like dementia. A very important finding is that different gait velocity parameters are associated with different cognitive domains, and therefore measuring the gait can be used to estimate which domain has a problem. A paper from 2018 [35] offers a very comprehensive review of diseases that can be detected with radar, and it also has many chapters on using radars indoors and signal processing techniques. However, the problem is that if mainly focuses on vitals monitoring instead of movement. A paper from 2014 [36] assesses the gait of people in home and mentions that it can be used for fall risk assessment, but does not implement it.

Overall, in the domain of diseases, gait estimation is a very popular topic, but the step from estimation to prediction has not been greatly explored. Many papers mention that the gait estimation compiled can be used for detecting diseases, but this is rarely implemented in practice.

3. Methodology

The project can be divided into two parts, where different datasets were used. However, a prior section has been added to explain the pre-processing of all the data. Both datasets contain range-time information, and spectrograms are created to be the source for features.

3.1. Pre-processing

The data taken from both datasets is a series of *'.dat'* files which contain a list of pairs of complex values. The first few lines show the parameters of the radar with which the data was captured, namely the center frequency, sweep time, number of samples per sweep and bandwidth. These are not only for information purposes, but also to assign correct labels to the axes of figures. The rest of the lines are pairs of complex values, which must undergo two different transformations.

3.1.1. Filtering.

An MTI filter must be applied to these values to discriminate the target against clutter [37]. What this means is that the filter is going to eliminate the signals that are received after bouncing against static objects, and solely keep the signals it obtains from moving objects. This is achieved by removing low frequency components. Static objects will return very low frequencies, and by applying a high-pass filter these will be eliminated. After this, the range-time plot can be shown. Figure 6 shows the same movement with and without an MTI filter.

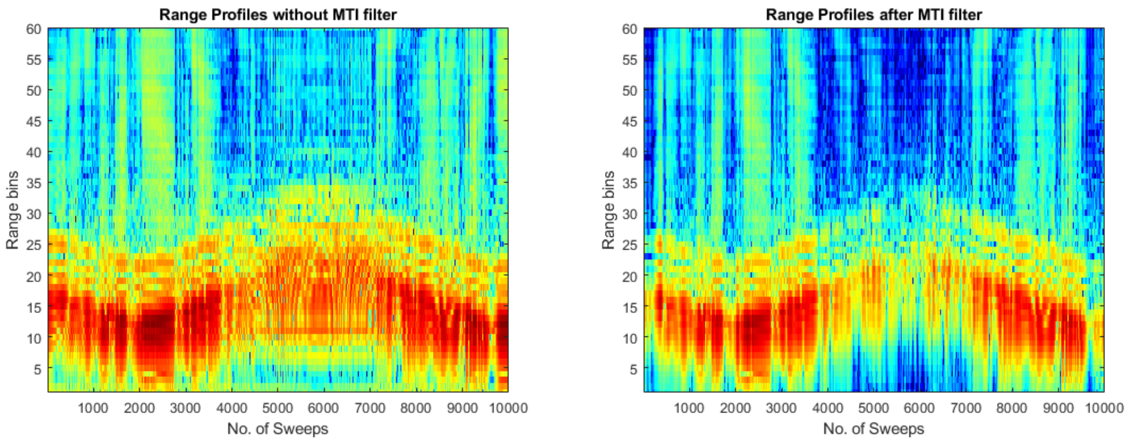

Figure 6: Range vs time with and without MTI

The movement can be appreciated in both, but the clutter is greatly reduced in the second image. For example, between 5000 and 7000 sweeps, in the plot without an MTI filter, there is a great amount of noise, which is then eliminated after the MTI filter. However, there is still some processing to be done.

3.1.2. Doppler vs time

The objective is to obtain a spectrogram of the movement the person is making [38]. After filtering the signal, a fast Fourier transform (FFT) is done to obtain the doppler vs time plot. A frequency shift must also be applied for the movement to be centered. The spectrogram is produced by repeating this FFT in many range bins, namely the ones where the movement is happening. In the case of the previous figure, the movement is probably happening between 5 and 25, so these limits should produce a reasonable spectrogram. Figure 7 shows the spectrograms with and without the original filter.

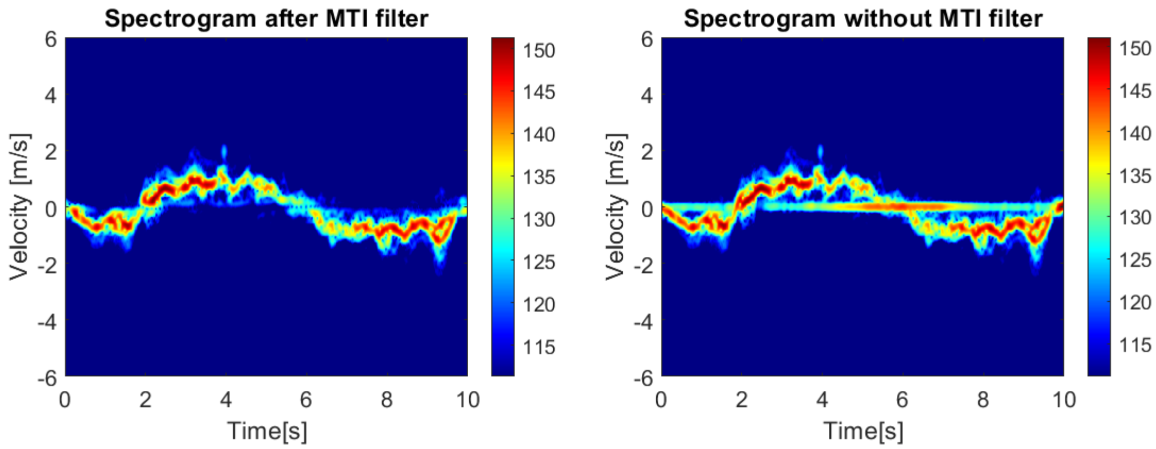

Figure 7: Spectrograms with and without MTI

The main difference is the line seen at 0m/s. This represents all the static objects that the radar captured, which are clearly not relevant to the analysis that is to be done. The filter serves its purpose and significantly improves the final spectrogram. Perhaps it is useful to explain exactly what is being seen on the spectrogram. From 0 to 2s the person is walking towards the radar, and from 2 to 6 away from it, then again towards it. If we analyze the movement from 2 to 6, the velocity of walk increases slowly until maximum to then decrease again until coming to a stop to turn around and continue the walk.

3.2. Classify movement

The first part of the project will use solely the Glasgow dataset. This contains people doing three repetitions of each of the six movements: walking, sitting down, standing up, bending down, drinking water and falling. The objective will be to classify each instance as one of these movements.

3.2.1. Extracting features

The ultimate purpose will be to perform machine learning to try and classify these movements, but it is unreasonable these files as they are into an algorithm and ask it to classify. To decrease the size of the model, it is vital to extract significant features from the spectrograms and use these to classify. Here is a list of all the features that were extracted from the spectrogram to be used

3.2.1.1. MFCC coefficients

Used in many papers ([39][40]) for feature extraction, it is based on extracting cepstral coefficients that contain information about the rate changes in different spectrum bands. In order to obtain them, the original signal must be split into short frames and then do the FFT for each of them. This eventually, after applying the Mel spectrum and a discrete cosine transform, will give a list of values. If a value is negative, that means that the majority of spectral energy is in the high frequencies, while if it is positive, it is concentrated in low-frequency.

3.2.1.2. Empirical features from spectrogram

Used in [41], three features are considered:

- Extreme frequency magnitude: maximum in absolute value between the maximum frequency in the positive frequency range and minimum in the negative.

$$F = \max\left(\text{abs}(f_{+max}, f_{-min})\right)$$

- Extreme frequency ratio:

$$R = \max\left(\left|\frac{f_{+max}}{f_{-min}}\right|, \left|\frac{f_{-min}}{f_{+max}}\right|\right)$$

- Length of event: The time from when the movement starts until it ends. This feature will be compiled without splitting the signal.

3.2.1.3. Statistical features from spectrogram

Every movement can be plotted as a single line which shows the location of the maximum value of the spectrogram for every column. From this line the features that can be extracted, after splitting the spectrogram, are the maximum, the minimum, mean and standard deviation. However, this approach is a bit reductionist, since a large amount of information is lost when the whole spectrogram is represented as a single line [42]. Therefore, these features should be used to support others, not by themselves. Figure 8 shows this line for a walking movement.

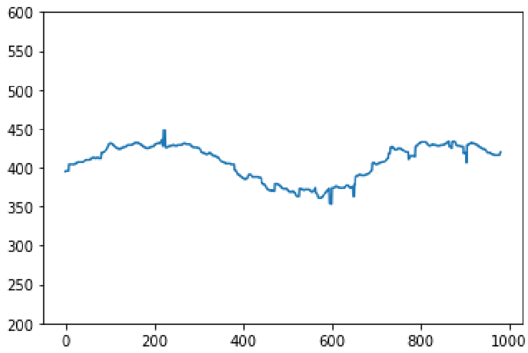

Figure 8: Line with maximum energy in spectrogram

3.2.1.4. Walking features

When the activity is walking, the spectrogram shows some distinct peaks that represent the movement of the legs [43]. Figure 9 shows these.

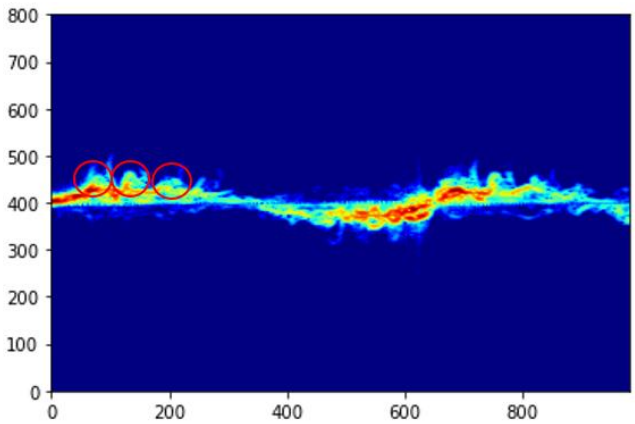

Figure 9: Legs in spectrogram

If these were isolated, it would be possible to compile some features based on their period and magnitude:

- Width ratio between odd and even leg cycles.

$$R = \max\left(\frac{T_{odd}}{T_{even}}, \frac{T_{even}}{T_{odd}}\right)$$

- Mean magnitude of intensity difference.

$$ID = (|\delta_1| + |\delta_2|)/2$$

  δ being the intensity differences between consecutive peaks of the limb signatures.

The clear problem here is that these features only exist when the activity is walking. Since the objective is to classify the movement, it wouldn't be known before extracting the features whether they will provide reasonable results or not. Therefore, it is of little use in this part of the project, but it will be very significant in the second part.

3.2.2. Change parameters to improve accuracy

Everything possible should be done to try and improve the accuracy of the model, from selecting features or which algorithm to use. This includes the way to preprocess and capture the data. There are two sets of parameters that can be changed: when doing the MTI filter and when compiling the spectrogram.

3.2.2.1. MTI

The main parameter that can be changed is the type of filter. Originally, a simple Butterworth filter is used [44]. However, the type of filter could affect the final accuracy of the algorithm, so others are tested, such as:

- Chebyshev [45]: allowing ripples, achieves a faster roll-off, and therefore offers a sharper transition between passband and stopband.
- Elliptic [46]: Has ripples both in passband and stopband, but has a steeper roll-off than Chebyshev.

Figure 10 shows these filters.

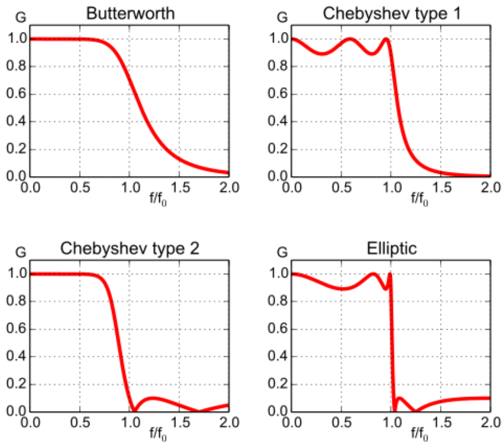

Figure 10: MTI filters

Apart from the type of filter, the parameters can also be changed, from the cutoff frequency to the peak-to-peak passband ripple.

3.2.2.2. Spectrogram

The main parameters that can be changed are:

- Overlap length between the FFT.
- Number of FFT points, which are based on the pad factor.
- Type of window to be applied. Originally, hamming window is chosen, but this could be changed to Blackman, Chebyshev, Gaussian… etc.

3.2.3. Perform classification

The first task that will involve a model is trying to classify the movements. As said before, the dataset contains 6 distinct movements, and the purpose of this first model is to classify each activity and assign it a label. Two approaches can be followed.

3.2.3.1. Machine Learning

The proposed algorithms for this are:

- Logistic regression [47]: the variables are used to create a regression curve and, using a sigmoid function, they are classified. Classical regression is not used due to the fact that all tasks are classification problems, not continuous estimations.
- K-nearest neighbors [48]: Every instance of the dataset is plotted in a n-dimensional plane (n being the number of variables). The labels of the k-closest points are studied to make predictions about the label of the point in question.
- Decision trees/ random forest [49]: A tree is created and the labels for every instance are filtered by the tree. A random forest is an ensemble algorithm in which many trees are created and the final label is chosen by majority voting.
- SVC (Support Vector Classification) [50]: Finds the best fitting hyperplane to divide the data.

3.2.3.2. Deep learning

Apart from these, there is a method that could bypass the previous step of feature extraction. This is using a CNN (Convolutional Neural Network) [51] and input the images into it. For this, the images of the spectrograms must be saved, then cropped to a standard size and input into the net.

The issue with neural nets, as is with all black boxes, is the lack of control [52]. When performing classical machine learning, the programmer can choose the features and evaluate what is happening much better, which is not always possible with a neural net. If the usage of the model is for a critical scenario, like prescribing medicine, a black box model is not suggested due to the lack of control over it.

The network design is that of a VGG [53]. The VGG has a very simple architecture primarily composed of convolutional layers stacked on top of each other, and reducing the size by max pooling. There is a degree of liberty when implementing this architecture, since the number of layers that can be stacked is up to the user. Two variations have been compared:

I. The first model has three sets of two-dimensional convolutional layer, which make the image 18x18 after the last layer. This is then flattened and densed to fit the number of classes being evaluated. Figure 11 shows the architecture.

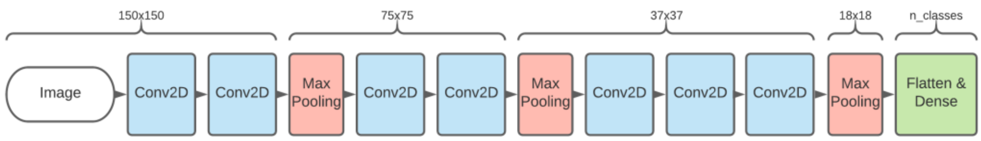

Figure 11: Fat VGG architecture

II. The second model is smaller, with one less convolutional layer to decrease computation time. This can be considered an ablation study to check if reducing the number of convolutional layers will greatly impact the performance. Figure 12 shows the architecture of this model.

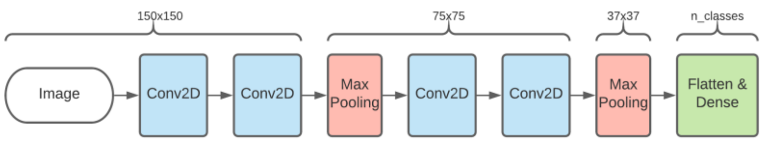

Figure 12: Simple VGG architecture

3.3. Evaluate movement

This second part of the project will use knowledge obtained from the Glasgow dataset to inform decisions in the design of a personalized monitoring system for patients. This monitoring system will contain a baseline movement for each person for every activity, which will be compared against which a new instance of that movement to estimate how similar they are. Figure 13 shows the flowchart for this process.

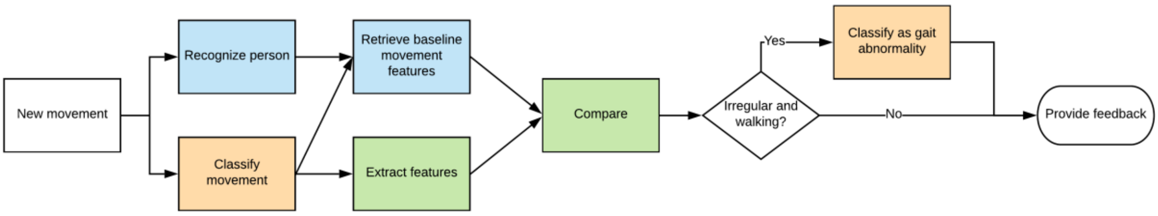

Figure 13: Flow chart of evaluating movement

The colors denote the operations. Orange are classifiers, green are the feature extraction and comparison and blue are the baseline movement.

3.3.1. Capture dataset

The first issue is scarceness of data. The dataset which was used for creating the classifier only contains up to three repetitions of every activity by each person. Some people participated again later in time, but very few of them. Therefore, more data needs to be created. The data collection is done by capturing 8 different people performing three activities in front of a radar: walking, sitting down and standing up. The reason for selecting these between the six that were available in the Glasgow dataset is the fact that this personalized system must be able to detect slight changes in how a person normally moves, and these were though to be the most representative of how a person moves.

However, irregularities of these activities will also be captured in order to have something that is not "normal" movement for each person. Irregularities mean that they will repeat the same movement but in an irregular way. For example, if the movement is standing up, the irregular way to do it would be by struggling to bring their weight up, if it's sitting down, they will put all their weight on one leg… etc. The most significant irregularities are for the walking movement. Stanford Medicine has made available a video where the most common gait abnormalities are demonstrated [54]. This is used to instruct test subjects to imitate these gait diseases, in order to add the functionality to the system of being able to recognize if a potential patient is suffering from one of these diseases. Therefore, a classifier is also trained to recognize between these gait diseases. More information about these can be found in the Appendix. Table 1 shows the activities that were captured for a single test subject. As said before, each activity had 3 repetitions. Apart from this, the radar used had 4 channels, so for every repetition, 4 files of data were created with slightly different values.

A1 (Walking)	*I0*
	I1 (Hemiplegic)
	I2 (Parkinsonian)
	I3 (Ataxic)
	I4 (Stomping)
	I5 (Spastic)

	I6 (Myopathic)
	I7 (Neuropathic)
A2 (Sitting down)	*I0*
	I1 (Put weight on leg)
	I2 (Let fall)
A3 (Stand up)	*I0*
	I1 (Put weight on leg)
	I2 (Put weight on arms)

Table 1: Captured dataset

3.3.2. Classifiers

Four different classifiers are trained. Figure 14 shows how they are interconnected. As for which features are used for each classifier, the conclusion extracted from the first part of the project with the Glasgow dataset are used to make informed decisions on how to combine or use these features.

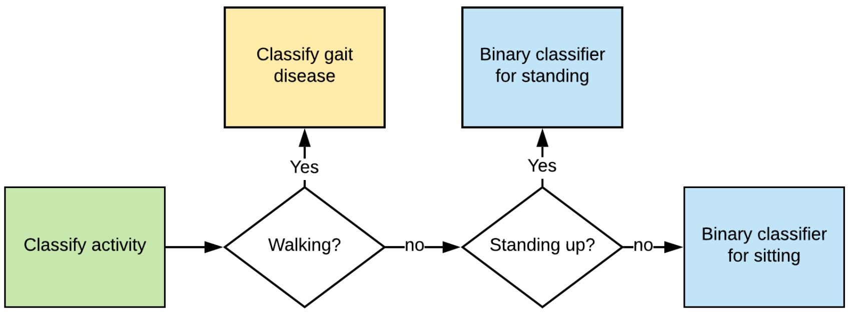

Figure 14: Flow chart of classifiers

3.3.2.1. Classify activity

This classifier has the same purpose as the one trained with the Glasgow dataset data: recognize which activity is taking place. Only three classes exist: walking, sitting down or standing up. The features considered are the same as for the first part of the project.

3.3.2.2. Classify gait disease

It was mentioned in section 3.2.1.4. that the walking features were of no use in the Glasgow dataset, but they would be in this part of the project. This classifier distinguishes between the gait diseases in walking, and uses the same features as the Glasgow dataset plus a few more:

1. Maximum speed of walk
2. Maximum speed of legs
3. Time between steps
4. Time of total movement

Figure 15 shows these four features on the spectrogram.

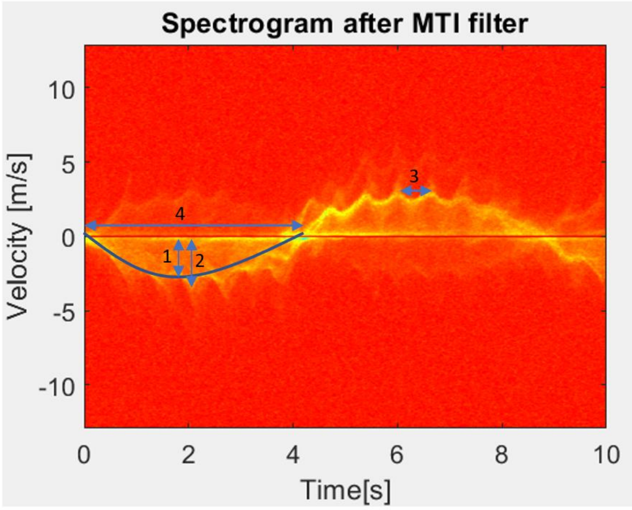

Figure 15: Walking features

3.3.2.3. Binary classifiers for standing and sitting

Although there are two irregularities for each movement as well as the baseline one, the classifiers are only trained to classify as normal or irregular movement. The features used as the same as the Glasgow dataset as well as:

1. Peak velocity
2. Dropoff
3. Length of event

Figure 16 shows these three on a sitting down and standing up spectrograms

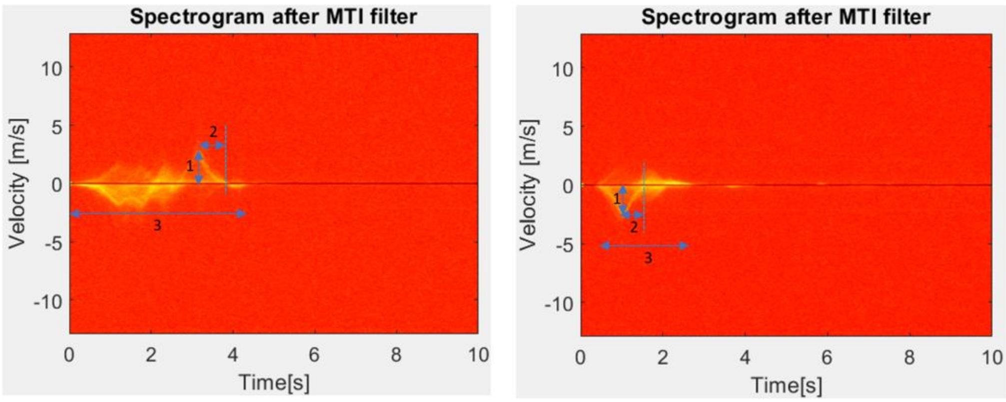

Figure 16: Sitting down (left) and standing up (right) features

3.3.3. Feature extraction and comparison

The features used for evaluating the movement are the ones described in the two previous sections. They are the same for sitting down and standing up, but they differ for walking. For this reason, before extracting features the movement will be classified as one of the three options, as discussed in 3.3.2.1. With this information, the features are extracted and compared against the features in the baseline movement of this person.

The baseline movement is formed from the “regular” movements for each person. It is important to note that the baseline movement is different for each person. Subject 1 might walk faster and have the time between steps be greater than that of subject 2, which means that each of their steps is bigger. Therefore, the features are extracted from the three repetitions (x4 because of the 4 channels in the radar), and the mean and standard deviation extracted. With this, if one of these features is outside of the limit $mean \pm 4 * std$, the feature is irregular and feedback is given to the subject. If the activity is walking, the movement will be classified as one of the gait diseases, showing which the walk is most similar to. Three files are saved, containing the baseline movement features for all the subjects, one file for every type of activity.

Assuming that all the features for each person follow a normal distribution, the reason for selecting 4 times the standard deviation is to account for slight changes to someone’s movement that however are not indicative of an irregularity. For example, if the person is more tired, their steps could be shorter or their walk might be slower, but this does not mean that they have an irregularity in their walk. 4 times the standard deviation accounts for 99.99% of the normal curve, so if one of the features is outside these limits, it can be assured that this is an irregularity. Figure 17 shows a normal distribution and how much the standard deviation limits account for.

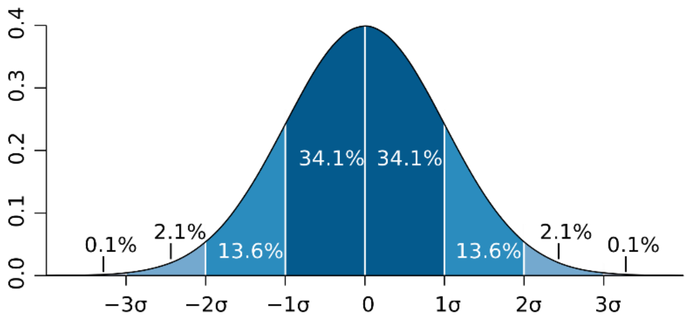

Figure 17: Normal distribution

4. Results and discussion

As mentioned before, this project can be divided into two parts: classification of movements in the Glasgow dataset and evaluation of movement with custom dataset. The results and discussion of them is outlined here, with an added section to explain how these results relate to one another.

4.1. Classify movement

The first part of the project is focused on extracting the features, classifying the movements and trying to improve the accuracy results by varying the parameters of how the spectrogram is created.

4.1.1. Extracting features

As mentioned in the corresponding section in methodology, there were a number of options considered for which features would be input into the model. Two sets of features were extracted and tested, as well as both sets together.

4.1.1.1. MFCC coefficients

The Mel spectral coefficients are compiled for every line of the spectrogram. Two considerations must be made:

- The lines are chosen instead of the columns of the spectrogram for extracting the coefficients due to the fact that different instances of activities are recorded for different periods of time. Figure 18 shows two activities, and as can be seen on the x axis, the duration is different.

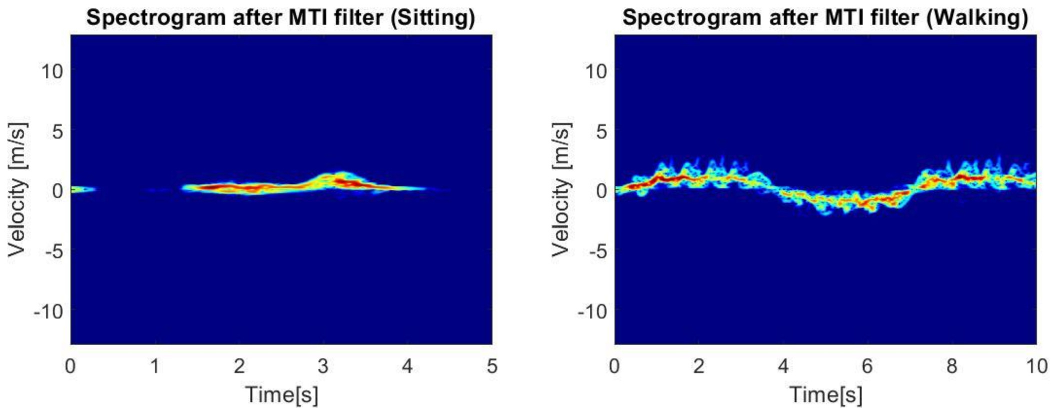

Figure 18: Sitting and walking spectrograms

  Since the sweep time is the same, the longer the duration, the more columns there will be. Therefore, to keep the number of features input into the model constant, and since the number of lines of the spectrogram is always the same, the Mel spectral coefficients are compiled for each line.

- The number of coefficients compiled for each line can be chosen. Therefore, different values are tested to see which provide the best accuracy.

Table 2 shows the accuracy scores for the models compiled with MFCC coefficients as features.

Features	Algorithm	Train	Test
MFCC **n=3200** **Coeff=3**	Logistic regression	1	0.86
	K-nearest	0.87	0.84
	Random forest	1	0.87

MFCC n= 4000 Coeff=4	Logistic regression	1	0.89
	K-nearest (k=1)	0.915	0.915
	Random forest	1	0.88
MFCC n= 4800 Coeff=5	Logistic regression	1	0.89
	K-nearest	0.9	0.9
	Random forest	1	0.87
MFCC n=8800 Coeff=10	Logistic regression	1	0.85
	K-nearest	0.89	0.85
	Random forest	1	0.84

Table 2: Accuracy scores for MFCC coefficients (Glasgow dataset)

The number of coefficients determined the number of features (n). It is interesting that the best results are not achieved by adding more and more features, but with a rather small number of 4 coefficients per line.

As it can be seen, the best results are achieved for K nearest neighbors with 4 coefficients. After hyperparameter tuning, the number of neighbors that provide this accuracy score is k=1. A problem commonly observed in this table is overfitting. Logistic regression and random forest provide a perfect training score, but quite a poor testing accuracy, while k nearest neighbors provides similar scores in train and test, independently of the number of coefficients.

When considering how this score could be improved without adding more features, it was considered that the top and bottom lines of the spectrogram don't provide any information about the type of movement, and therefore are just noise. If features have no importance, as would logically be the case for these lines, eliminating them could provide a better accuracy score. Therefore, the MFCC coefficients were compiled again, but instead of ranging from -10m/s to 10m/s, only the lines from -5m/s to 5m/s were considered. Table 3 shows the accuracy scores for these new coefficients.

Features	Algorithm	Train	Test
MFCC n=1600 Coeff=3	Logistic regression	1	0.87
	K-nearest	1	0.87
	Random forest	1	0.89
MFCC n= 2000 Coeff=4	Logistic regression	1	0.88
	K-nearest (k=1)	0.923	0.923
	Random forest	1	0.89
MFCC n= 2400 Coeff=5	Logistic regression	1	0.87
	K-nearest	0.91	0.89
	Random forest	1	0.87

Table 3: Accuracy scores for MFCC coefficients (smaller spectrogram)

Clearly, the scores are improved, achieving a 1% increase to the maximum accuracy while reducing the features to half. To better observe which classes are being confused, the confusion matrix is compiled and shown in Figure 19.

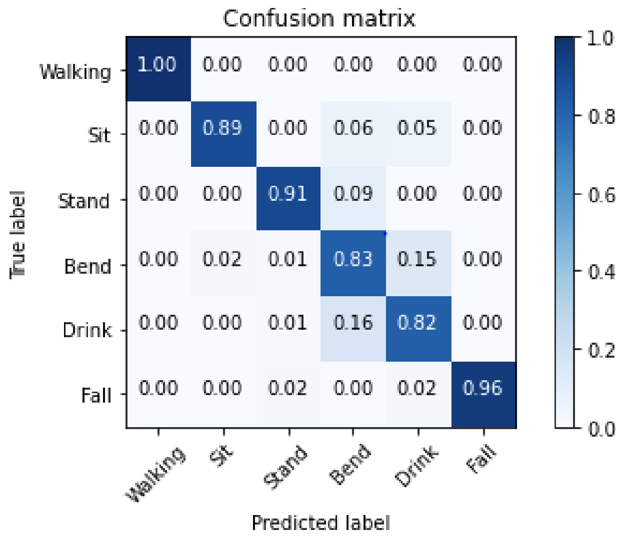

Figure 19: Confusion matrix for MFCC features

Very satisfactory results, with only two classes with high confusion between them: bending and drinking. All other classes have decent accuracy, with a 100% for walking being especially impressive.

4.1.1.2. Main line

Following and combining the features explained in sections 3.2.1.2 and 3.2.1.3, the "main line", as it will be called from now on, is the line of maximum energy in the spectrogram. This line is split into n parts, and for each section, the maximum, minimum, mean and standard deviation are compiled. The number of sections determines the number of features that will be input into the model. An extra feature is added labelled "length", which represents the duration of the activity, by assessing if there is a point with significantly more energy in every column of the spectrogram. If this is not the case, it is considered that there is no activity in this column. Table 4 shows the accuracy results with these features.

Features	Algorithm	Train	Test
Main line	Logistic regression	0.8	0.7
n=41	K-nearest (k=2)	0.93	0.84
Sections=10	Random forest	1	0.84
Main line	Logistic regression	0.72	0.67
n=21	K-nearest	0.75	0.55
Sections=5	Random forest	1	0.67
Main line	Logistic regression	0.78	0.62
n=61	K-nearest	0.69	0.57
Sections=15	Random forest	1	0.66

Table 4: Accuracy of main line features

It was considered relevant to observe how the added feature of "length" improves the accuracy. Table 5 shows the best performing features without the length.

Features	Algorithm	Train	Test
Main line **n=40** **Sections=10**	Logistic regression	0.7	0.6
	K-nearest	1	0.82
	Random forest	1	0.84

Table 5: Accuracy of main line without length

As it can be seen, the improvement is most noticeable with the logistic regression algorithm, while also contributing to k nearest neighbours.

The confusion matrix is also compiled for the main line features, and it can be seen in Figure 20.

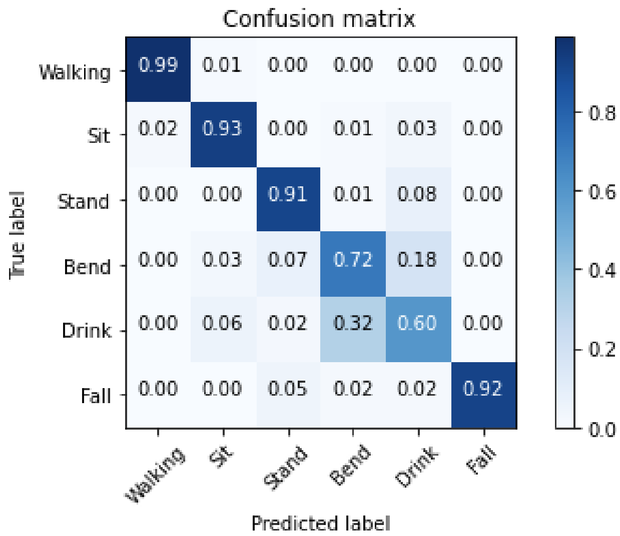

Figure 20: Confusion matrix for main line

Clearly, the classes that are bringing down the classifier are bending and drinking water, as there is a large amount of confusion between them. All other classes have an accuracy in the 90s, and specially distinguishing the walking class achieved a very high accuracy of 99%. Similar results to the ones obtained with FMCC coefficients, only higher confusion between the two classes mentioned.

4.1.1.3. MFCC + Main line

Using the MFCC coefficients provides better results than the main line, although the number of features is also much greater. Combining both sets of features is the next logical step. Only the best performing features are combined. Table 6 shows the results for each algorithm

Features	Algorithm	Train	Test
Main line +MFCC **n= 2041**	Logistic regression	1	0.85
	K-nearest	0.91	0.9
	Random forest	1	0.86

Table 6: Accuracy of combined features

The results show that the results improve on the ones obtained solely with the main line, but do not improve on the MFCC features score. Therefore, it can be concluded that the best features for this specific dataset are the MFCC coefficients.

4.1.1.4. Without MTI filter

As explained in section 3.1.1., the first step when pre-processing the dataset is to apply an MTI filter to eliminate the low frequency components. This was done as it was considered that it would provide better classification results, since it reduces the clutter. To justify this choice, the best performing features have been extracted from the spectrograms without applying the aforementioned MTI filter. Table 7 shows the results for the classification task.

Features	Algorithm	Train	Test
Main line	Logistic regression	0.41	0.41
n=41	K-nearest	0.61	0.45
Sections=10	Random forest	0.53	0.48
MFCC	Logistic regression	1	0.88
n=2000	K-nearest	1	0.89
Coeff=4	Random forest	1	0.88

Table 7: Accuracy without MTI filter

A few conclusions can be extracted from this:

- The line of maximum energy offers very little information, as if the low frequency components are not eliminated, most of the energy is concentrated around the 0 Doppler line. Therefore, the length feature will be the same for all instances, since the energy has a significantly high point for every column of the spectrogram, as seen in Figure 21.

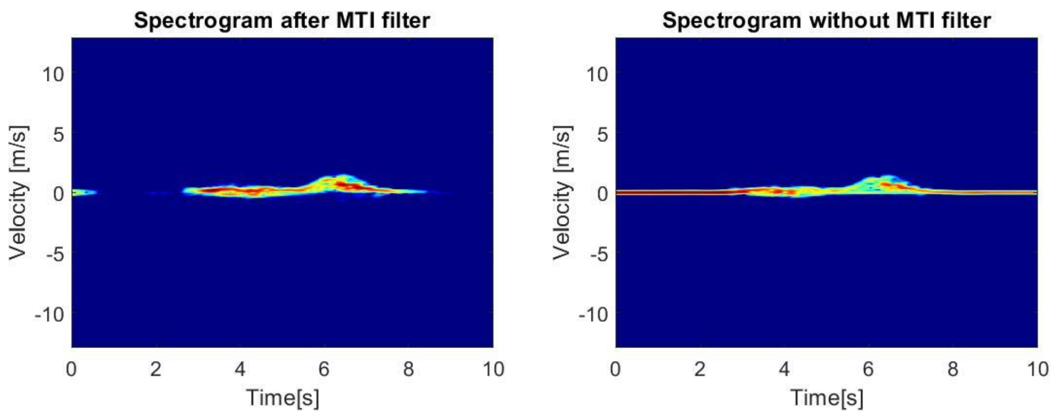

Figure 21: Activity with and without MTI filter

- The MFCC coefficients provide similar, while slightly lower, results, since the only information being lost is near the 0 Doppler line.

4.1.2. Change parameters

As explained in the Methodology section, in an effort to improve the accuracy of the classifier, different parameters have been changed when compiling the spectrogram. Two sets of parameters could be changed, depending on if they were relevant to the MTI filter or to the creation of the spectrogram itself.

4.1.2.1. MTI

Three parameters were meant to be varied to test which provides the best accuracy: type of filter, cut-off frequency and peak-to-peak passband ripple. Since the main difference when using MTI and not is seen in the accuracy for the main line features, it was compared how changing these parameters affects the accuracy for the model that has these features. However, when testing the difference between filters, it could be seen that it did not impact the model accuracy significantly. This can be seen in Table 8.

Filter	Algorithm	Train	Test
Butterworth	Logistic regression	0.8	0.7
	K-nearest	0.93	0.84
	Random forest	1	0.84
Chebyshev	Logistic regression	0.79	0.71
	K-nearest	0.93	0.84
	Random forest	1	0.83
Elliptic	Logistic regression	0.81	0.7
	K-nearest	0.92	0.83
	Random forest	1	0.83

Table 8: Accuracy with different filters

The only function of the filter is to eliminate the low frequency components, that is, the static objects in the frame. It can either achieve this, or leave some remnants, depending on the cut-off frequency more than the type of filter or passband ripple. If the spectrogram does not show the heavy energy line around the 0 Doppler, this means that the filter achieved its objective and eliminated these components. If these is some energy around that line, it did not. Therefore, if the correct cut-off frequency can be found, the filter choice will not impact the model significantly. Table 9 shows spectrograms with different cut-off frequencies (order of magnitude) and their accuracy.

Cut-off	Spectrogram	Algorithm	Train	Test
10^{-3}	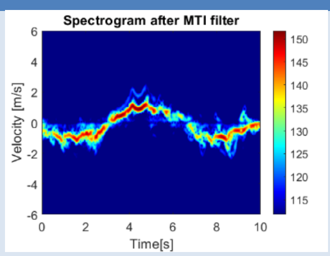	Logistic regression	0.8	0.7
		K-nearest	0.93	0.84
		Random forest	1	0.84

10^{-2}	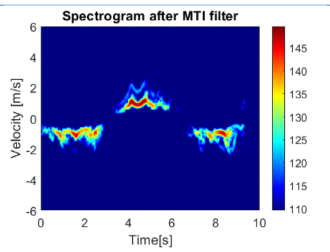	Logistic regression	0.45	0.4
		K-nearest	0.51	0.45
		Random forest	0.43	0.4
10^{-4}	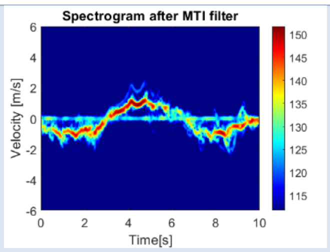	Logistic regression	0.6	0.55
		K-nearest	0.71	0.63
		Random forest	0.73	0.6

Table 9: Accuracy with cut-off frequencies

As it can be seen in the accuracy and the spectrogram, the best performing is at an order of magnitude of 10^{-3}.

4.1.2.2. Spectrogram

Three parameters are varied and tested on the best performing features:

I. Overlap length

Overlap length	Train	Test
100	0.9	0.89
150	0.91	0.91
200	0.92	0.92

Table 10: Accuracy with overlap

II. Pad factor

Pad factor	Train	Test
3	0.91	0.9
4	0.92	0.92
5	91	0.91

Table 11: Accuracy with pad factor

III. Type of window

Window	Train	Test
Hamming	0.92	0.92
Blackman	0.92	0.91
Chebyshev	0.92	0.91

Table 12: Accuracy with window type

With this, the best performing parameters are overlap length of 200, pad factor of 4 and Hamming window. The results are very similar for all, but a slight improvement is noticeable with these parameters.

4.1.3. Deep learning

Apart from extracting these features and performing classical machine learning models on them, in parallel, when their spectrograms were being compiled, a picture of them was being saved in order to be input into a CNN network. Two versions of a CNN network were created, simple and fat, with the fat having more convolutional layers. The images were processed in order to crop the to not include the axes, as these existed for all images and didn't provide any information, so the only thing input to the network would be the spectrograms themselves. The results can be seen in Table 13.

Net	Epochs	Train	Validation	Test
VGG simple	7	0.932	0.92	0.91
VGG fat	21	0.915	0.917	0.918

Table 13: CNN accuracy

The simple VGG net need much less epochs than the fat one to deliver similar results. Therefore, the simple VGG performs best in this scenario.

4.2. Evaluate movement

As explained before, a custom dataset was developed for the second part of the project. Four classifiers were trained.

4.2.1. Activity classifier

The conclusions extracted from the Glasgow dataset as to how to extract features to perform the classification tasks was utilized here. The first impression after looking at the confusion matrices for the previous section is that the model that will classify the activity will achieve a very high accuracy, since the two classes that were bringing the overall score down are no longer present. With this, Table 14 shows the accuracy scores.

Features	Algorithm	Train	Test
MFCC n=6400 Sections=3	Logistic regression	1	0.998
	K-nearest	1	0.98
	Random forest	1	0.997
Main line + length n=9 Sections=2	Logistic regression	0.998	0.997
	K-nearest	1	0.995
	Random forest	1	0.995

Table 14: Accuracy of activity classifier

The testing was cut short, as there was no need to look for any better classifiers. By splitting the spectrogram in 2 and finding the main line, while also using the length feature, the accuracy is near perfect and no further testing was needed.

4.2.2. Walking classifier

The classifier to find which type of irregularity the walking movement is associated with has 7 classes: regular, hemiplegic, ataxic, stomping, spastic, myopathic and neuropathic. Many features were tested, which can be found in Table 15.

Features	Algorithm	Train	Test
MFCC n=9600 Coeff=5	Logistic regression	1	0.93
	K-nearest	0.86	0.74
	Random forest	1	0.93
MFCC n=6400 Coeff=3	Logistic regression	1	0.87
	K-nearest	0.94	0.87
	Random forest	1	0.89
MFCC n=3200 Coeff=3	Logistic regression	1	0.91
	K-nearest	1	0.99
	Random forest	1	0.93
Main line n=17	Logistic regression	0.7	0.6
	K-nearest	1	0.96

Sections=3	Random forest	1	0.95
Main line	Logistic regression	0.5	0.5
n=9	K-nearest	1	0.9
Sections=2	Random forest	1	0.93

Table 15: Accuracy of walking classifier

While many features provide good accuracy results, the best are achieved by the MFCC with 3 coefficients on the cropped spectrogram, as it was for the Glasgow dataset in the first part of the project.

4.2.3. Binary classifiers

Two classifiers were trained: one for the sitting down movement and one for standing up.

I. Sit down: Table 16 shows the accuracy results.

Features	Algorithm	Train	Test
MFCC	Logistic regression	1	1
n=9600	K-nearest	1	1
Coeff=5	Random forest	1	1
MFCC	Logistic regression	1	1
n=6400	K-nearest	1	1
Coeff=3	Random forest	1	0.95
MFCC	Logistic regression	1	0.71
n=3200	K-nearest	1	0.91
Coeff=3	Random forest	1	0.64
Main line	Logistic regression	0.68	0.64
n=17	K-nearest	1	0.83
Sections=3	Random forest	1	0.78
Main line	Logistic regression	0.6	0.6
n=9	K-nearest	1	0.66
Sections=2	Random forest	1	0.7

Table 16: Accuracy of sit classifier

An interesting situation arises. For the first time, better results are achieved when the spectrogram is not cropped. This is surprising, as it means that some information is hidden in the very high frequencies. This is confirmed by the main line accuracy, which is much lower. The main line is a reductionist approach that discards all information in the high frequencies, and only focuses on the line of maximum energy. Since the accuracy is so low, it shows that some important information is being left out.

II. Stand up: Table 17 shows the accuracy results.

Features	Algorithm	Train	Test
MFCC **n=9600** **Coeff=5**	Logistic regression	1	0.86
	K-nearest	0.86	0.86
	Random forest	1	0.74
MFCC **n=6400** **Coeff=3**	Logistic regression	1	0.86
	K-nearest	0.94	0.86
	Random forest	1	0.81
MFCC **n=3200** **Coeff=3**	Logistic regression	1	0.69
	K-nearest	1	0.79
	Random forest	1	0.62
Main line **n=17** **Sections=3**	Logistic regression	0.92	0.87
	K-nearest	1	0.95
	Random forest	1	0.87
Main line **n=9** **Sections=2**	Logistic regression	0.8	0.73
	K-nearest	1	0.76
	Random forest	1	0.8

Table 17: Accuracy of stand classifier

This model has the worst accuracy of the three, but it is obtained with the fewest features. A main line with 3 sections offers a 95% test accuracy.

4.2.4. Feature extraction

The features are different for walking and the other two movements, so they will be explained in different sections.

4.2.4.1. Walking movement

The features described in the Methodology section have to be extracted. For this purpose, a new line is compiled, which will from now be called "limit line". This limit line represents the movement of the fastest component for every chirp. Figure 22 shows an example of this line for a walking movement.

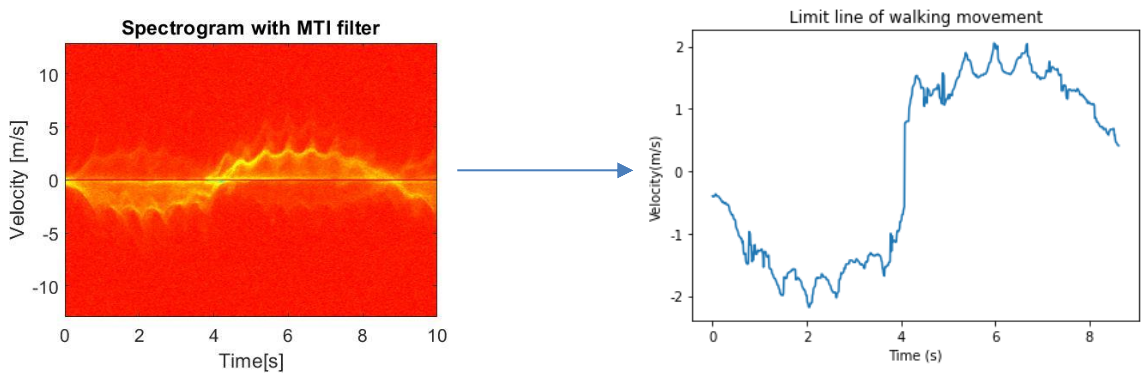

Figure 22: Spectrogram to limit line

As it can be seen, it is called “limit line” because it represents the limits of the person’s movement, where the leg movement can be seen very clearly. However, the limit line is not compiled for all 10 seconds of movement. Instead, the movement is sectioned into “complete” walks. A complete walk is considered the entire movement of going from the starting position (5m away from the radar) to the radar, or from the radar to the starting position. Most people walking without an irregularity have time to do 2 complete walks in 10 seconds, with few exceptions depending on the speed of walk. However, when an irregularity is present people tend to move more slowly, not being able to complete 2 walks. Therefore, the features are extracted from only complete walks. If there is more than one in a single movement, the features are extracted for each and then averaged. Figure 23 shows these complete walks for two different walks: one without irregularity and one with.

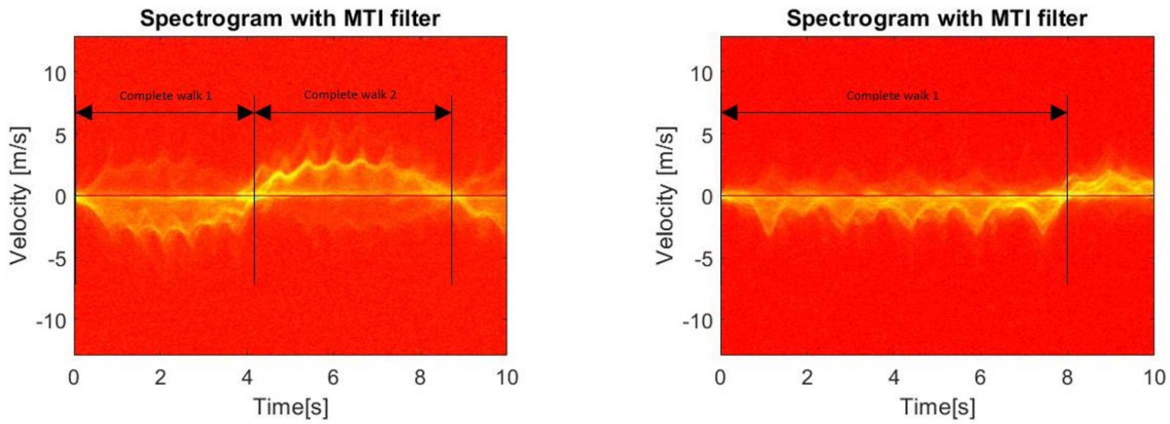

Figure 23: Complete walks without irregularity (left) and with (right)

The next step to extract the features is find maximums and minimums. Every point of the limit line is compared with its neighbours to check if it is the maximum or minimum. The number of neighbours to compare is crucial, as if the number is too small, many points that will be mislabelled as maximums or minimums, or if it is too big, some of the points could be omitted. Experimentally, the numbers that were found to provide the most accurate results were comparing with 15-18 neighbours on each side. Figure 24 shows the limit line with maximums and minimums.

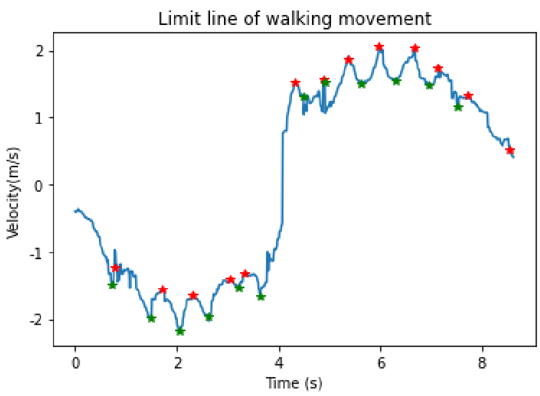

Figure 24: Maximums and minimums of limit line

Most points correspond to the maximums and minimums, but a few are mislabelled. This is remedied when the features are being compiled, by eliminating outliers that don't match up with the rest of the values.

The process to extract every feature is explained here:

I. **Maximum speed of walk:**
The walk is the movement of the body. This is represented by the maximums when the velocity is smaller than 0 and the minimums when the velocity is greater than 0. The maximum in absolute value of these is compiled, and if there are two complete movements, the average is calculated.

II. **Maximum speed of legs:**
The legs are represented by the minimums when velocity is smaller than 0 and by maximums when velocity is greater than 0. Again, the maximum in absolute value is calculated and if there are two complete movements, the average.

III. **Time between steps:**
The distance between minimums when velocity smaller than 0 and maximums when greater than 0. Outliers are eliminated and the average is calculated.

IV. **Time of total movement:**
The time of one complete movement. If there is more than 1, take the average.

4.2.4.2. Other movements

The feature extraction for sitting down and standing up is very similar, and will be explained in this section. The limit line is compiled again for each movement. Since now there is only one movement, the line represents the full 10 seconds. Figure 25 shows the limit line for each movement.

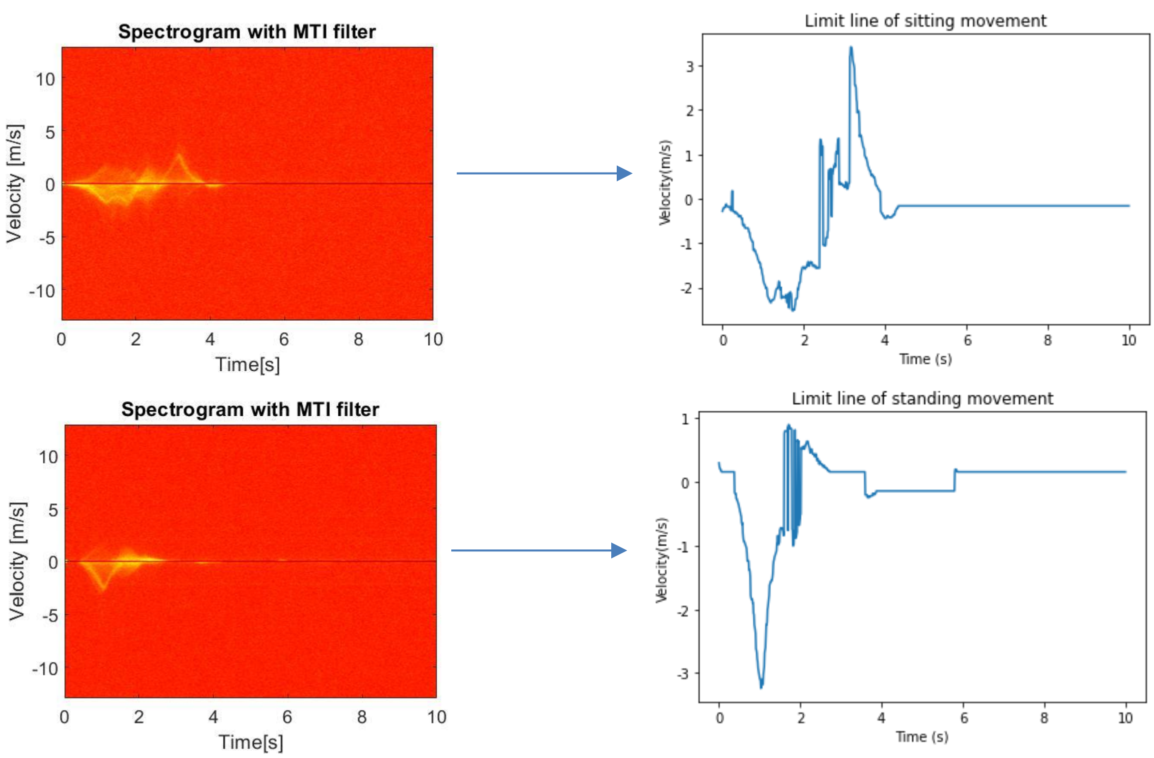

Figure 25: Limit line for sitting and standing

It is important to say that for the sitting movement, the actual sitting action does not start immediately. In the graph shown it starts around the 3 second mark. Until then the person is walking from to side of the chair to the front. Therefore, this part is not relevant and the features concentrate on the period after this. The three features for both movements are:

I. **Peak velocity**
The maximum for sitting and minimum for standing.
II. **Dropoff**
The time it takes from the peak velocity to back to 0.
III. **Length of event**
Time where movement is detected.

4.2.4.3. Feature comparison

For every person, the features for every movement are stored in a dataframe. Every person has 12 spectrograms for their regular movements (3 repetitions with 4 channels). The average and standard deviation are calculated and then stored in three dataframes, one for each movement. Figure 26 shows an example of one of these dataframes.

Person	Irregularity	Dist_steps	Peak_walk	Peak_legs	Len_move	std_steps	std_walk	std_legs	std_len
1	0	55.051902	176.291667	223.875000	411.041667	4.598082	14.289949	8.842370	17.862427
2	0	51.180255	163.416667	212.833333	440.625000	4.632874	9.100033	11.215520	8.942048
3	0	57.376213	182.666667	243.000000	342.500000	4.674112	9.286680	12.871745	19.594758
4	0	51.633131	190.833333	237.875000	359.833333	6.271616	21.669347	12.542881	5.955644
5	0	59.881432	157.708333	200.750000	455.208333	2.296912	9.550008	6.853997	25.238371
6	0	66.010660	119.000000	162.833333	469.750000	6.183889	6.944586	3.386694	33.757491
7	0	59.132912	178.583333	242.041667	399.458333	4.054341	15.626076	27.782809	26.494818
8	0	53.362262	212.875000	269.208333	339.888889	2.701350	10.034316	8.843226	9.849712

Figure 26: Walking dataframe

As it was predicted, every person has slightly different features, so a personalized evaluation is the best approach, instead of a general baseline for everyone. Person 6 for example walks much slower than Person 4, as seen by their “peak_walk” feature. While Person 4 walks faster than Person 3, the legs of Person 3 move faster than those of Person 4. With this, for every new instance of a movement, the features are extracted and compared against these.

4.2.5. All together

To demonstrate the functionality of the system, an instance of an activity will be put through the pipeline. All the steps are explained.

1. Capture movement and extract spectrogram, after applying MTI filter. Figure 27 shows the completed spectrogram.

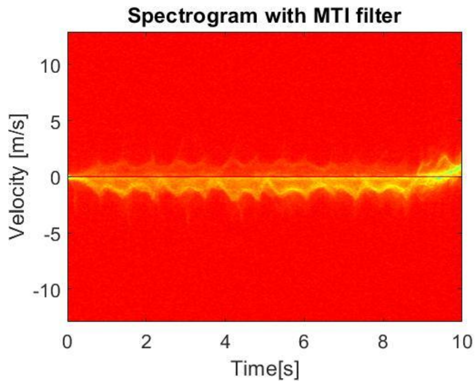

Figure 27: Spectrogram of example

2. The first task is to classify the type of activity. The main line is extracted and its statistical features input into the model. The classifier recognizes this as a walking activity.
3. Extract walking features from the spectrogram. Figure 28 shows the limit line with maximums and minimums.

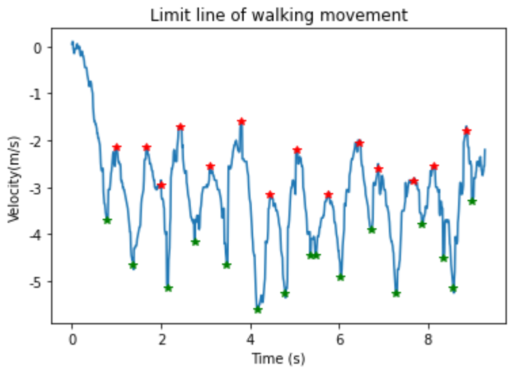

Figure 28: Limit line of example

As explained before, only complete movements are used to extract features, hence why the length of the limit line is not the full 10s. The features are compiled from this limit line.

4. Retrieve baseline movement features for this person from dataframe.
5. Compare baseline movement features and extracted features. The system output is:

```
The time between your steps is normal
The speed of your walk is lower than normal
The speed of your legs is lower than normal
It took you longer than usual to walk this distance
```

6. Since some features are outside of the norm (speed of walk, speed of legs and time of movement) and the activity is walking, the walking classifier is used to estimate which gait disease this movement resembles the most. The MFCC coefficients from the cropped spectrogram are obtained and the classifier recognizes this as a Neuropathic gait.

5. Conclusions and further work

Each part of the project had its own conclusions, so they will be explained separately.

5.1. Classify movement

The main purpose of this task was to extract conclusion to be used in the second one. The questions it aimed to answer were:

- What features provide the best classification scores?
- Which parameters when creating the spectrogram provide the best scores?
- Is deep learning a suitable approach?

All of these were answered, finding that MFCC and main line features were valuable and provided high scores, being the features compared in the second part of the project. The best parameters were also found, and the results of the CNN were to be similar to those of classical machine learning approaches, while much more computationally expensive, discarding this method as a suitable one for the task in hand.

5.2. Evaluate movement

As the main novel part of the project, the results from this section were more important than the first one. The accuracy of all classifiers proved that using the MFCC coefficients and the main line features was an appropriate approach to the task. The final system was able to detect changes in a person's movement by extracting solely 4 features, and the walking classifier to recognize gait diseases provided a very high accuracy. The approach of using a different baseline movement for each person proved to be correct, as it was seen that the walks of people were varied and the features extracted from their movements differed.

5.3. Further work

The many possible applications of this project have been outlined earlier, but what was developed was quite a generic function of simply comparing to see if there is a difference in movements. For each of them, a more specific system could be designed to automate the processes described. A system is proposed for each.

- At home monitoring: Keep track of patients at home, they would have to perform the movements in front of a radar once in a while. If the movement was not irregular, the movement features should be weighted and added to the baseline movement.
- Athletes: Same as for at home monitoring, perhaps with an added functionality to include more movements. For example, a footballer could track his progress when shooting. Features could be extracted from the movement, like range of leg, speed of leg… etc. They could be used to track if a player improves over time, and could include other parameters like the speed of the ball, direction… etc to rate his skills.
- Physiotherapy: Since the movement after suffering an injury or being in physiotherapy would be irregular, the system would have the baseline on file and could quantify how far from it every instance is.
- Diseases: The proposed system predicts the most common gait diseases, but this could be improved to include more gait diseases, or even different diseases that could be predicted by the movement.

6. References

[1] Diraco, G., Leone, A., & Siciliano, P. (2017). A Radar-Based Smart Sensor for Unobtrusive Elderly Monitoring in Ambient Assisted Living Applications. *Biosensors*, *7*(4), 55. https://doi.org/10.3390/bios7040055

[2] M. G. Amin, Y. D. Zhang, F. Ahmad and K. C. D. Ho, "Radar Signal Processing for Elderly Fall Detection: The future for in-home monitoring," in IEEE Signal Processing Magazine, vol. 33, no. 2, pp. 71-80, March 2016, doi: 10.1109/MSP.2015.2502784.

[3] Fioranelli, Francesco & Syed, Aziz & Shah, Syed Aziz & Li, Haobo & Shrestha, Aman & Yang, Shufan & Julien, Dr & le kernec, Julien. (2019). Radar Sensing for Healthcare. Electronics Letters. 10.1049/el.2019.2378.

[4] Mcewan, Body Monitoring And Imaging Apparatus And Method,Us Patent 5,766,208, June 16, 1998

[5] Øyvind Aardal and Jan Hammerstad 2010 Medical radar literature overview Norwegian Defence Research Establishment (FFI) rapport 2010/00958

[6] Pisa, Stefano & Pittella, Erika & Piuzzi, Emanuele. (2016). A Survey of Radar Systems for Medical Applications. IEEE Aerospace and Electronic System Magazine. 31. 10.1109/MAES.2016.140167.

[7] James, Mihir & Vala, Alpesh & Patel, Amit & Patel, Hitesh. (2018). A Brief Review on Bio-Medical Application of Radar.

[8] Silva Girão, Pedro & Postolache, O. & Postolache, Gabriela & Ramos, Pedro & Pereira, J. (2015). Microwave Doppler radar in unobtrusive health monitoring. Journal of Physics: Conference Series. 588. 10.1088/1742-6596/588/1/012046.

[9] Xu Y, Lu YH, Zhang HX, Wang YQ 2007 An overview of ultra-wideband technique application for medial engineering Proc. IEEE/ICME Int. Conf. Complex Med. Eng. 408-411 Beijing PR China

[10] E. M. Staderini, "UWB radars in medicine," in IEEE Aerospace and Electronic Systems Magazine, vol. 17, no. 1, pp. 13-18, Jan. 2002, doi: 10.1109/62.978359.

[11] Hamelmann, Paul & Vullings, Rik & Kolen, Alexander & Bergmans, Jan & van Laar, Judith & Tortoli, Piero & Mischi, Massimo. (2019). Doppler Ultrasound Technology for Fetal Heart Rate Monitoring: A Review. IEEE Transactions on Ultrasonics, Ferroelectrics, and Frequency Control. PP. 1-1. 10.1109/TUFFC.2019.2943626.

[12] Michael Otero, "Application of a continuous wave radar for human gait recognition," Proc. SPIE 5809, Signal Processing, Sensor Fusion, and Target Recognition XIV, (25 May 2005); https://doi.org/10.1117/12.607176

[13] Z. Zhang, Z. Tian and M. Zhou, "Latern: Dynamic Continuous Hand Gesture Recognition Using FMCW Radar Sensor," in IEEE Sensors Journal, vol. 18, no. 8, pp. 3278-3289, 15 April15, 2018, doi: 10.1109/JSEN.2018.2808688.

[14] Z. Peng, C. Li, J. Muñoz-Ferreras and R. Gómez-García, "An FMCW radar sensor for human gesture recognition in the presence of multiple targets," 2017 First IEEE MTT-S International Microwave Bio Conference (IMBIOC), Gothenburg, Sweden, 2017, pp. 1-3, doi: 10.1109/IMBIOC.2017.7965798.

[15] O. Postolache, P. S. Girão, R. N. Madeira and G. Postolache, "Microwave FMCW Doppler radar implementation for in-house pervasive health care system," 2010 IEEE International Workshop on Medical Measurements and Applications, Ottawa, ON, Canada, 2010, pp. 47-52, doi: 10.1109/MEMEA.2010.5480207.

[16] T. G. Stavropoulos, G. Meditskos, S. Andreadis and I. Kompatsiaris, "Real-time health monitoring and contextualised alerts using wearables," *2015 International Conference on Interactive Mobile Communication Technologies and Learning (IMCL)*, 2015, pp. 358-363, doi: 10.1109/IMCTL.2015.7359619.

[17] Mielnik, Pawel & Tokarz, Krzysztof & Mrozek, Dariusz & Czekalski, Piotr & Fojcik, Marcin & Hjelle, Anja & Milik, Mateusz. (2019). Monitoring of Chronic Arthritis Patients with Wearables - A Report from the Concept Phase. 10.1007/978-3-030-28374-2_20

[18] Diraco, G., Leone, A., & Siciliano, P. (2017). A Radar-Based Smart Sensor for Unobtrusive Elderly Monitoring in Ambient Assisted Living Applications. *Biosensors*, *7*(4), 55. https://doi.org/10.3390/bios7040055

[19] Figueroa, Adrian & Al-Qudsi, Belal & Joram, Niko & Ellinger, Frank. (2016). Comparison of two-way ranging with FMCW and UWB radar systems. 1-6. 10.1109/WPNC.2016.7822856.

[20] C. E. Phillips et al., "Radar walk detection in the apartments of elderly," 2012 Annual International Conference of the IEEE Engineering in Medicine and Biology Society, 2012, pp. 5863-5866, doi: 10.1109/EMBC.2012.6347327.

[21] Boroomand, Ameneh & Shaker, George & Morita, Plinio & Wong, Alexander & Boger, Jennifer. (2018). Autonomous Gait Speed Estimation Using 24GHz FMCW Radar Technology. 10.1109/BHI.2018.8333371.

[22] M. G. Amin, Y. D. Zhang, F. Ahmad and K. C. D. Ho, "Radar Signal Processing for Elderly Fall Detection: The future for in-home monitoring," in IEEE Signal Processing Magazine, vol. 33, no. 2, pp. 71-80, March 2016, doi: 10.1109/MSP.2015.2502784.

[23] B. Erol, M. G. Amin, B. Boashash, F. Ahmad and Y. D. Zhang, "Wideband radar based fall motion detection for a generic elderly," 2016 50th Asilomar Conference on Signals, Systems and Computers, 2016, pp. 1768-1772, doi: 10.1109/ACSSC.2016.7869686.

[24] B. Jokanovic, M. Amin and F. Ahmad, "Radar fall motion detection using deep learning," 2016 IEEE Radar Conference (RadarConf), 2016, pp. 1-6, doi: 10.1109/RADAR.2016.7485147.

[25] Onks, Cayce & Hall, Donald & Ridder, Tyler & Idriss, Zacharie & Andrie, Joseph & Narayanan, Ram. (2021). The Accuracy and Predictability of Micro Doppler Radar Signature Projection Algorithm Measuring Functional Movement in NCAA Athletes. Gait & Posture. 85. 96–102. 10.1016/j.gaitpost.2021.01.021.

[26] C. Glaros, D. I. Fotiadis, A. Likas and A. Stafylopatis, "A wearable intelligent system for monitoring health condition and rehabilitation of running athletes," 4th International IEEE EMBS Special Topic Conference on Information Technology Applications in Biomedicine, 2003., 2003, pp. 276-279, doi: 10.1109/ITAB.2003.1222531.

[27] Seshadri, D.R., Li, R.T., Voos, J.E. *et al.* Wearable sensors for monitoring the physiological and biochemical profile of the athlete. *npj Digit. Med.* **2,** 72 (2019). https://doi.org/10.1038/s41746-019-0150-9

[28] D. R. Seshadri, C. Drummond, J. Craker, J. R. Rowbottom and J. E. Voos, "Wearable Devices for Sports: New Integrated Technologies Allow Coaches, Physicians, and Trainers to Better Understand the Physical Demands of Athletes in Real time," in IEEE Pulse, vol. 8, no. 1, pp. 38-43, Jan.-Feb. 2017, doi: 10.1109/MPUL.2016.2627240.

[29] O. Postolache, "Remote sensing technologies for physiotherapy assessment," 2017 10th International Symposium on Advanced Topics in Electrical Engineering (ATEE), 2017, pp. 305-312, doi: 10.1109/ATEE.2017.7905141.

[30] T. Martins, V. Carvalho and F. Soares, "Application for physiotherapy and tracking of patients with neurological diseases - Preliminary studies," 2013 IEEE 2nd International Conference on Serious Games and Applications for Health (SeGAH), 2013, pp. 1-8, doi: 10.1109/SeGAH.2013.6665317.

[31] Burns D, Razmjou H, Shaw J, Richards R, McLachlin S, Hardisty M, Henry P, Whyne C Adherence Tracking With Smart Watches for Shoulder Physiotherapy in Rotator Cuff Pathology: Protocol for a Longitudinal Cohort Study JMIR Res Protoc 2020;9(7):e17841

[32] K. Saho, M. Fujimoto, M. Masugi and L. Chou, "Gait Classification of Young Adults, Elderly Non-Fallers, and Elderly Fallers Using Micro-Doppler Radar Signals: Simulation Study," in IEEE Sensors Journal, vol. 17, no. 8, pp. 2320-2321, 15 April15, 2017, doi: 10.1109/JSEN.2017.2678484.

[33] Yang, Le & Li, Gang & Ritchie, Matthew & Fioranelli, Francesco & Griffiths, Hugh. (2016). Gait Classification Based on Micro-Doppler Features. 10.1109/RADAR.2016.8059301.

[34] K. Saho, K. Uemura, K. Sugano and M. Matsumoto, "Using Micro-Doppler Radar to Measure Gait Features Associated With Cognitive Functions in Elderly Adults," in IEEE Access, vol. 7, pp. 24122-24131, 2019, doi: 10.1109/ACCESS.2019.2900303.

[35] Amin, M. (2018). *Radar for indoor monitoring*. Boca Raton: CRC Press.

[36] F. Wang, M. Skubic, M. Rantz and P. E. Cuddihy, "Quantitative Gait Measurement With Pulse-Doppler Radar for Passive In-Home Gait Assessment," in IEEE Transactions on Biomedical Engineering, vol. 61, no. 9, pp. 2434-2443, Sept. 2014, doi: 10.1109/TBME.2014.2319333.

[37] Karmakar, Priyabrata & Dhar, Sourav & Chakraborty, Mithun & Paul, Tirthankar. (2013). Comparative Study of Four Different Types of MTI Filters for Radar Clutter Rejection. International Journal of Image, Graphics and Signal Processing. 5. 40-46. 10.5815/ijigsp.2013.05.05.

[38] French, Mark & Handy, Rod. (2007). Spectrograms: Turning Signals into Pictures. Journal of Engineering Technology. 24. 32-35.

[39] J. Hong, S. Tomii, and T. Ohtsuki, “Cooperative fall detection using Doppler radar and array sensor,” in Proc. IEEE 24th Annu. Int. Symp. Pers., Indoor, Mobile Radio Commun. (PIMRC), Sep. 2013, pp. 3492–3496

[40] S. Tomii and T. Ohtsuki, “Falling detection using multiple Doppler sensors,” in Proc. IEEE 14th Int. Conf. e-Health Netw., Appl. Services, Healthcom, Oct. 2012, pp. 196–201.

[41] L. R. Rivera, E. Ulmer, Y. D. Zhang, W. Tao, and M. G. Amin, “Radarbased fall detection exploiting time-frequency features,” in Proc. IEEE China Summit Int. Conf. Signal Inf. Process. (ChinaSIP), Jul. 2014, pp. 713–717.

[42] Lampert, Thomas & O'Keefe, Simon. (2010). A Survey of Spectrogram Track Detection Algorithms. Applied Acoustics. 71. 87-100. 10.1016/j.apacoust.2009.08.007.

[43] Ahmad, Fauzia & Amin, Moeness & Boashash, Boualem & Zhang, Yimin. (2015). Human gait recognition with cane assistive device using quadratic time–frequency distributions. IET Radar, Sonar & Navigation. 9. 10.1049/iet-rsn.2015.0119.

[44] Bansal, Mohit. (2010). Performance evaluation of Butterworth Filter for Signal Denoising. 10.13140/RG.2.1.4809.8161.

[45] Podder, Prajoy & Hasan, Md. Mehedi & Islam, Md & Sayeed, Mursalin. (2020). Design and Implementation of Butterworth, Chebyshev-I and Elliptic Filter for Speech Signal Analysis.

[46] F. Ali, R. Jain, D. Gupta and A. Agarwal, "Design and Analysis of Low Pass Elliptic Filter," 2016 Second International Conference on Computational Intelligence & Communication Technology (CICT), 2016, pp. 449-451, doi: 10.1109/CICT.2016.95.

[47] Bewick, Viv & Cheek, Liz & Ball, Jonathan. (2005). Statistics review 14: Logistic regression. Critical care (London, England). 9. 112-8. 10.1186/cc3045.

[48] Cunningham, Padraig & Delany, Sarah. (2007). k-Nearest neighbour classifiers. Mult Classif Syst.

[49] Breiman, L. Random Forests. Machine Learning 45, 5–32 (2001). https://doi.org/10.1023/A:1010933404324

[50] Evgeniou, Theodoros & Pontil, Massimiliano. (2001). Support Vector Machines: Theory and Applications. 2049. 249-257. 10.1007/3-540-44673-7_12.

[51] Krizhevsky, Alex & Sutskever, Ilya & Hinton, Geoffrey. (2012). ImageNet Classification with Deep Convolutional Neural Networks. Neural Information Processing Systems. 25. 10.1145/3065386.

[52] Zednik, Carlos. (2021). Solving the Black Box Problem: A Normative Framework for Explainable Artificial Intelligence. Philosophy & Technology. 34. 10.1007/s13347-019-00382-7.

[53] Simonyan, Karen & Zisserman, Andrew. (2014). Very Deep Convolutional Networks for Large-Scale Image Recognition. arXiv 1409.1556.

[54] D. Goyal, K. Rao Jerripothula and A. Mittal, "Detection of Gait Abnormalities caused by Neurological Disorders," 2020 IEEE 22nd International Workshop on Multimedia Signal Processing (MMSP), 2020, pp. 1-6, doi: 10.1109/MMSP48831.2020.9287163.

7. Appendix: Gait diseases

The University of Stanford has made available a video with the most common gait abnormalities. The descriptions are as follows (taken directly from [54]):

- Hemiplegic gait: The patient stands with unilateral weakness on the affected side, arm flexed, adducted and internally rotated. Leg on same side is in extension with plantar flexion of the foot and toes. When walking, the patient will hold his or her arm to one side and drags his or her affected leg in a semicircle (circumduction) due to weakness of distal muscles (foot drop) and extensor hypertonia in lower limb. This is most commonly seen in stroke. With mild hemiparesis, loss of normal arm swing and slight circumduction may be the only abnormalities.
- Parkinsonian: In this gait, the patient will have rigidity and bradykinesia. He or she will be stooped with the head and neck forward, with flexion at the knees. The whole upper extremity is also in flexion with the fingers usually extended. The patient walks with slow little steps known at marche a petits pas (walk of little steps). Patient may also have difficulty initiating steps. The patient may show an involuntary inclination to take accelerating steps, known as festination. This gait is seen in Parkinson's disease or any other condition causing parkinsonism, such as side effects from drugs.
- Ataxic: Most commonly seen in cerebellar disease, this gait is described as clumsy, staggering movements with a wide-based gait. While standing still, the patient's body may swagger back and forth and from side to side, known as titubation. Patients will not be able to walk from heel to toe or in a straight line. The gait of acute alcohol intoxication will resemble the gait of cerebellar disease. Patients with more truncal instability are more likely to have midline cerebellar disease at the vermis.
- Stomping: As our feet touch the ground, we receive propioreceptive information to tell us their location. The sensory ataxic gait occurs when there is loss of this propioreceptive input. In an effort to know when the feet land and their location, the patient will slam the foot hard onto the ground in order to sense it. A key to this gait involves its exacerbation when patients cannot see their feet (i.e. in the dark). This gait can be seen in disorders of the dorsal columns (B12 deficiency or tabes dorsalis) or in diseases affecting the peripheral nerves (uncontrolled diabetes). In its severe form, this gait can cause an ataxia that resembles the cerebellar ataxic gait.
- Spastic: Patients have involvement on both sides with spasticity in lower extremities worse than upper extremities. The patient walks with an abnormally narrow base, dragging both legs and scraping the toes. This gait is seen in bilateral periventricular lesions, such as those seen in cerebral palsy. There is also characteristic extreme tightness of hip adductors which can cause legs to cross the midline referred to as a scissors gait. In countries with adequate medical care, patients with cerebral palsy may have hip adductor release surgery to minimize scissoring.
- Myopathic: Hip girdle muscles are responsible for keeping the pelvis level when walking. If you have weakness on one side, this will lead to a drop in the pelvis on the contralateral side of the pelvis while walking (Trendelenburg sign). With bilateral weakness, you will have dropping of the pelvis on both sides during walking leading to waddling. This gait is seen in patient with myopathies, such as muscular dystrophy.
- Neuropathic: Seen in patients with foot drop (weakness of foot dorsiflexion), the cause of this gait is due to an attempt to lift the leg high enough during walking so that the foot does not drag on the floor. If unilateral, causes include peroneal nerve palsy and L5 radiculopathy. If bilateral,

causes include amyotrophic lateral sclerosis, Charcot-Marie-Tooth disease and other peripheral neuropathies including those associated with uncontrolled diabetes.